Standard Reference Material 2036 Near-Infrared Reflection Wavelength Standard*

STEVEN J. CHOQUETTE,† DAVID L. DUEWER, LEONARD M. HANSSEN, and EDWARD A. EARLY‡

Analytical Chemistry Division, Chemical Science and Technology Laboratory (S.J.C., D.L.D.), and Optical Technology Division, Physics Laboratory (L.M.H., E.A.E.), National Institute of Standards and Technology, Gaithersburg, Maryland 20899-8394

Standard Reference Material 2036 (SRM 2036) is a certified transfer standard intended for the verification and calibration of the wavelength/wavenumber scale of near-infrared (NIR) spectrometers operating in diffuse or trans-reflectance mode. SRM 2036 *Near-Infrared Wavelength/Wavenumber Reflection Standard* is a combination of a rare earth oxide glass of a composition similar to that of SRM 2035 *Near-Infrared Transmission Wavelength/Wavenumber Standard* and SRM 2065 *Ultraviolet–Visible–Near-Infrared Transmission Wavelength/Wavenumber Standard,* but is in physical contact with a piece of sintered poly(tetrafluoroethylene) (PTFE). The combination of glass contacted with a nearly ideal diffusely reflecting backing provides reflection–absorption bands that range from 15% *R* to 40% *R*. SRM 2036 is certified for the 10% band fraction air wavelength centroid location, $^{10\%}$B, of seven bands spanning the spectral region from 975 nm to 1946 nm. It is also certified for the vacuum wavenumber $^{10\%}$B of the same seven bands in the spectral region from 10 300 cm^{-1} to 5130 cm^{-1} at 8 cm^{-1} resolution. Informational values are provided for the locations of thirteen additional bands from 334 nm to 804 nm.

Index Headings: **SRM 2036; Standard reference material; Wavelength standard; Wavelength calibration; Reflectance spectroscopy; Near-infrared; Diffuse reflectance; Optical filters.**

INTRODUCTION

Several participants involved in a 1998 inter-laboratory comparison of Standard Reference Material (SRM®) 2035, *Near Infrared Transmission Wavelength Standard*, requested data for the use of this standard in a ''quasi''-diffuse reflectance mode. Several users placed SRM 2035 in physical contact with Spectralon® (Labsphere, North Sutton, NH), a proprietary sintered poly(tetrafluoroethylene) material, and measured the combination in a trans-reflectance mode to calibrate the wavelength axis of their fiber-optic probes. Based upon industry recommendations, comments from the U.S. Food and Drug Administration, and the dearth of useable calibration methods for sphere-based instruments, NIST decided to investigate the certification of an SRM 2035-style optical filter for diffuse reflectance. The result is Standard Reference Material 2036 *Near-Infrared Wavelength/Wavenumber Reflection Standard.* This optical filter is a certified transfer standard intended for the verification and calibration of the wavelength/wavenumber scale of near-infrared (NIR) spectrometers operating in diffuse or trans-reflectance mode.

In the early 1980s, the optical technology division of NIST developed SRM 1920a *Near Infrared Reflectance Wavelength Standard from 740 nm to 2000 nm* for the calibration of low resolution spectrometers in the NIR. SRM 1920a is a physical mixture of the three neat rare earth oxides (REO) of dysprosium, erbium, and holmium. The mixture provides over 37 certified absorption bands in the spectral region from 800 nm to 2100 nm, at spectral slit resolutions ranging from 2 nm to 10 nm. However, since the absorption bands of the neat REOs are extremely narrow, tend to overlap, and have apparent locations that depend on instrument resolution, the certified locations of these bands have approximate 95% confidence intervals, U_{95}, of 1 nm. Because it was the only standard available, SRM 1920a became the *de facto* industry standard for the calibration of NIR instruments used in the pharmaceutical and agricultural industries. Unfortunately, these applications frequently require lower uncertainties, certification at higher resolution than the current 2 nm slit spectral width limitation, less dependence of the band position on instrument resolution, and, for Fourier transform (FT) instruments, certification of the band locations in wavenumbers rather than wavelength.

SRM 2036 was originally intended to complement SRM 1920a. However, recently secondary standards vendors have initiated the production of SRM-1920a-style surrogates. The band locations and other optical properties of the SRM-1920a-style physical mixture using FT instruments[1,2] have recently been published. As a result, many of the limitations of SRM 1920a have been addressed by the academic and instrument vendor communities. Because of the commercial acceptance of this standard and the availability of materials from secondary standards vendors, SRM 1920a will no longer be produced by NIST. Those laboratories requiring traceability to NIST will be served by SRM 2036. Producing SRM 2036 from the same glass formulation as SRMs 2035 and 2065 has the advantage that they share the same approximate band locations and temperature coefficients and are readily available from a commercial supplier.[3] The methods and procedures used to certify SRM 2036 are similar to those used for SRM 2035 and SRM 2065.[4–6] The Certificates of Analysis of these two SRMs as well as that for SRM 2036 may be viewed on-line.[7–9]

EXPERIMENTAL

Spectrum. The reflectance spectrum of SRM 2036 measured at 5 nm spectral slit width (SSW) is shown in

Received 27 October 2004; accepted 7 December 2004.

* Certain commercial equipment is identified to specify adequately the experimental procedure. Such identification does not imply a recommendation or endorsement by the National Institute of Standards and Technology, nor does it imply that the equipment is the best available for the purpose.

† Author to whom correspondence should be sent. E-mail: steven.choquette@nist.gov.

‡ Currently with AFRL/HEDO, Brooks City-Base, TX.

0003-7028/05/5904-496$2.00/0

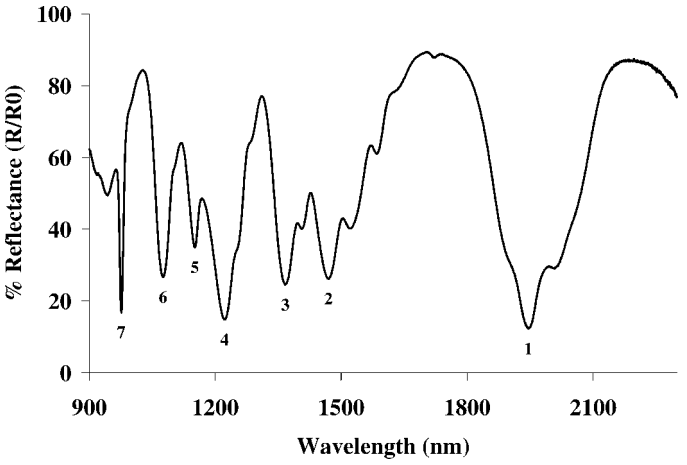

FIG. 1. SRM 2036 measured at 5 nm spectral slit width.

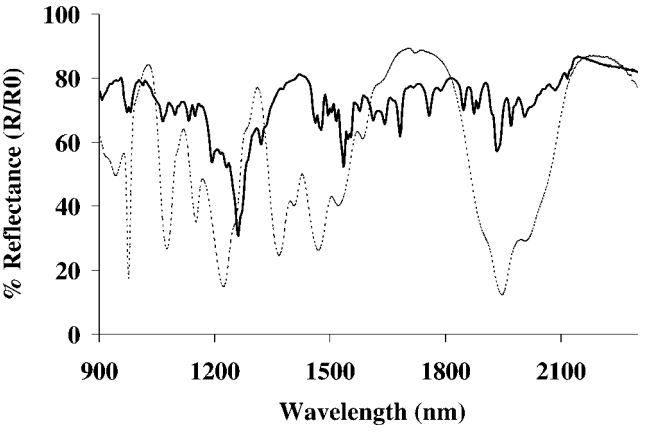

FIG. 2. Comparison of SRM 1920a (solid) and SRM 2036 (dotted).

Fig. 1 over the region from 900 nm to 2400 nm. A similarly acquired spectrum of SRM 1920a, and for comparison, SRM 2036, is shown in Fig. 2.

Materials. SRM 2036 raw material was provided to NIST as a custom melt by Schott Glass North America (Duryea, PA). This glass contains 3.00% mole fraction holmium oxide (Ho_2O_3), 1.30% mole fraction samarium oxide (Sm_2O_3), 0.68% mole fraction ytterbium oxide (Yb_2O_3), and 0.47% mole fraction neodymium oxide (Nd_2O_3) in a zirconia-stabilized borate glass containing lanthanum oxide (La_2O_3). All rare earth oxide purities exceeded 99.9%. NIST optical shop personnel machined the glass block into 25 mm diameter disks of 1.5 mm nominal thickness.

The sintered PTFE was obtained from Hudson Valley Optics (Wilmington, OH). Each piece was machined to a tolerance of 0.995 in. +.000/−.010 diameter by 0.240 in. ± 0.005 in. thickness. The sintered PTFE is held in physical contact with the glass disk by a 25 mm diameter optical mount (LH1-100R) obtained from Newport Corporation (Irvine, CA).

Reference Fourier Transform Near-Infrared Spectrometer Measurements. The spectrometers used for the determination of the vacuum wavenumber band locations of SRM 2036 were a Bruker IFS66 Fourier Transform spectrometer and a BioRad FTS-60A spectrometer interfaced to a custom-designed integrating sphere accessory. The Bruker spectrometer is equipped with a tungsten light source, silicon-coated CaF_2 beamsplitter, and a choice of liquid-nitrogen-cooled InSb, room temperature germanium, or thermoelectrically cooled InGaAs detectors. The BioRad FTS-60A is equipped with a wide-range, liquid-nitrogen cooled HgCdTe detector, a TiO_2 coated quartz beamsplitter and a tungsten light source. Both the Bruker and BioRad systems were purged with dry nitrogen.

The Bruker system was utilized for the homogeneity, stability, temperature coefficients, fiber-optic probe, and transmission experiments (without diffuse reflection backing). This instrument was equipped with a Pike Technologies six-position autosampler (Madison, WI) mounted in an external temperature-controlled sampling unit. The temperature of the external unit was maintained at 25 °C ± 1 °C using passive radiative heating/cooling with a refrigerated water bath. Data on this system were typically acquired as 256 double-sided, coadded forward and backward scans of the interferometer at 8.0 cm^{-1} resolution. An internal beam aperture of 1.0 mm was used to ensure adequate collimation of the source. Spectrally neutral wire mesh screens were used to attenuate the beam to ensure linear detector response. The interferometer scan speed of 20 kHz was optimized for the InSb detector. Mertz phase correction and a Norton–Beer three-term apodization function were applied to the raw interferograms. The resulting interferogram was then zero-filled by a factor of eight, yielding a data interval of 0.97 cm^{-1}. Each filter measurement had a separate air/PTFE reference measurement, taken under identical instrument conditions. The resulting interferogram data were converted to absorbance/reflectance versus wavenumber spectra using a commercial software routine (Opus ver. 3.1).

For the fiber probe measurements, an Axiom Analytical (Los Angles, CA) fiber probe assembly was interfaced to the Bruker IFS66. This sample accessory was placed within the sample chamber of the spectrometer and does not appreciably affect the purge of the instrument. The probe is a bifurcated fiber optic with 1 mm illumination and collection fiber bundles. The probe head utilizes a random mixture of these fibers. Although not ideal for diffuse reflectance sampling (an arrangement of collection fibers around a central illumination fiber would reject the specular component of the sample), it is representative of the types of probes commonly used in the field.

The BioRad FTS-60A integrating sphere/FT system was utilized for the determination of the absolute directional-hemispherical reflectance of the SRM 2036 glass/sintered PTFE sandwich combination. The integrating sphere was mounted in an externally purged chamber. Details of this spectrometer and custom integrating sphere can be found in Ref. 10. Reflectance data were collected in both specular-included (8° incidence) and diffuse-only or specular-excluded (0° incidence) geometries for both SRM 2036 and a reference sample of PTFE. Data were collected as a double-sided interferogram, using the Mertz phase correction method. All single channel spectra (sample and reference) were collected as 1024 co-additions at 8 cm^{-1} nominal constant wavenumber resolution. A total of 24 reflectance measurements of each sample were averaged to increase the signal-to-noise ratio

and to reduce error due to drift. Additionally, one data set included half-beam blocks to assess the potential for band location bias due to inter-reflection between the sample and interferometer.

The sphere itself rotates between sample and reference positions. In the reference position, the beam enters the sphere in a manner that is equivalent to a reflection off a perfect specular reflector mounted in the reference port. The sample reflectance position is achieved by a combined rotation of the sphere about two axes. In this position, the beam enters the entrance port and illuminates the sample mounted (from the outside) on the opposite wall of the sphere. The ratio of measurements made in the two positions provides a direct absolute reflectance for a specular sample or an absolute reflectance for a diffuse sample that includes multiplication by a calibration spectrum. The sphere calibration spectrum accounts for the spatial variations in sphere throughput averaged for a perfect diffuser. This correction is linear and is approximately 10% at 10 000 cm^{-1}.

Frequency Calibration of the Fourier Transform Spectrometers. The Bruker IFS 66 spectrometer in the Analytical Chemistry Division (ACD) was calibrated using both atmospheric water vapor and SRM 2517 *High Resolution Wavelength Calibration Reference for 1510 nm–1540 nm Acetylene* $^{12}C_2H_2$. SRM 2517 is an acetylene (C_2H_2) gas optical-fiber-coupled absorption cell intended for calibration of instruments in the wavelength range between 1510 nm to 1540 nm.[11] The peak locations of fifty absorption lines of the R and P branches of the $\upsilon 1 + \upsilon 3$ rotational–vibrational bands of C_2H_2 are certified with expanded uncertainty of 0.0006 nm (0.003 cm^{-1}). This NIR wavelength standard is intended primarily for the calibration of wavelength division multiplexers used in optical fiber communication. The absorption spectrum of SRM 2517 was measured by positioning the gas cell at the point of focus of the near-infrared beam. Water vapor was measured by briefly breaking the purge of the spectrometer. Spectra were acquired as 16 coadded scans at 0.125 cm^{-1} resolution with boxcar apodization of the interferogram. The spectra were post-zero-filled by a factor of four, giving a final data interval of 0.031 cm^{-1} for the resulting transmittance spectra.

Water lines were compared to literature values.[12] These rotational–vibration bands are centered between 5141 cm^{-1} to 5507 cm^{-1} and 7135 cm^{-1} to 7355 cm^{-1}. The line positions of SRM 2517 are located between these bands, at 6561 cm^{-1} to 6605 cm^{-1}. Although calibration of FT spectrometers is typically a single point calibration process, for purposes of the certification of this SRM the entire R branch (22 observed lines) of the acetylene standard was used. The average peak differences were calculated between the Bruker FT spectrometer and the certified vacuum wavelength values to determine an average correction to be applied to the HeNe frequency of the FT spectrometer. This correction factor was used to calibrate the frequency axis of the Bruker spectrometer to the *vacuum wavenumber* scale.

The corrected water-vapor spectra were then compared to literature values for corroboration of the calibration. The average offset of the water and C_2H_2 lines before calibration was 0.026 cm^{-1} (standard deviation = 0.005 cm^{-1}). After calibration, the average difference for the 22 observed R branch lines for 19 measurements of SRM 2517 over 10 days was 0.0033 cm^{-1} with a standard deviation of 0.0046 cm^{-1}. No drift or appreciable change in calibration was noted during the duration of the filter certification.

The BioRad FTS-60A spectrometer was calibrated with water vapor lines in the regions around 5250 cm^{-1} and 3000 cm^{-1}. Four lines were found and compared to the literature values.[12] The correction factor was calculated as the average of the ratio of the found H_2O lines $V_{\text{literature}}/V_{\text{measured}}$. This average correction, b, was then used to correct the wavenumber axis using

$$V_{\text{corrected}} = b \times V_{\text{measured}}$$

After calibration, the average residual difference between the literature and corrected spectra was -0.07 cm^{-1}.

Dispersive Ultraviolet–Visible–Near-Infrared Spectrometer Measurements. The air-wavelength-band locations of SRM 2036 were measured with a Varian Cary 5e, dispersive UV-Visible-NIR spectrometer and compared to similar measurements on a PerkinElmer Lambda-900 (PE900) spectrometer. The PE900 spectrometer was equipped with a 60 mm integrating sphere (PELA 1020, Labsphere, North Sutton, NH) accessory with internal PbS and photomultiplier detectors. The Cary was equipped with a 110 mm sphere and similar detectors. Sample spectra of SRM 2036 and PTFE reference samples were acquired in both specular-included (8° wedge angle) and specular-excluded (diffuse-only) modes. Samples of SRM 2036 were randomly selected from the lot and were measured at 3 nm, 5 nm, and 10 nm spectral slit width with a 0.5 nm data point spacing from 900 nm to 2300 nm. Sample integration times were 0.5 s per data point. Each reflectance spectrum of the SRM was ratioed to a calibrated PTFE reference spectrum. The sample temperature ranged from 22 °C to 27 °C during these experiments.

Ultraviolet–visible measurements of SRM 2036 were performed on the PE900 spectrometer with the PELA 1020 integrating sphere accessory. Spectra were acquired from 320 nm to 880 nm with a 5 nm spectral slit width (SSW) and 0.2 nm data point spacing.

Wavelength Calibration of the Dispersive Instruments. Because integrating spheres are not optically efficient, traditional methods of wavelength calibration using emission pen lamps are difficult, if not impossible. Both instruments were wavelength calibrated using the internal deuterium lamp and the vendor software. This utilizes the 656.1 nm band in the second order of the grating (1312.2 nm). Hg pen lamps can be used to give data out to approximately 1500 nm when using the 253.7 nm line in the third through sixth orders, but systematic errors and declining signal intensity reduce the utility of this approach. For this certification SRM 2065 (used in transmission before the sphere) and SRM 1920a (measured on the sphere in diffuse reflectance) were used in addition to the D_2 lines to provide calibration of these instruments. Validation of the calibration on the PE900 was also assessed using neat liquid samples of chloroform contained in 1 mm path length cuvettes. First-order combination bands of this compound give sharp bands in the 2000 nm to 2500 nm region. Chloroform was measured from 4 cm^{-1} to 64 cm^{-1} constant wavenumber res-

TABLE I. SRM 2036 homogeneity assessment. All values in cm^{-1}.

	SRM 2035[a]		SRM 2036[b]					
			Run 1		Run 2		Run 3	
Band	$\bar{X}$	$u(\bar{X})$[c]	$\bar{X}$	$u(\bar{X})$[c]	$\bar{X}$	$u(\bar{X})$[c]	$\bar{X}$	$u(\bar{X})$[c]
1	5138.50	0.02	5138.41	0.02	5138.40	0.02	5138.44	0.02
2	6804.90	0.06	6804.48	0.04	6804.48	0.05	6804.41	0.04
3	7313.30	0.32	7312.95	0.07	7312.93	0.10	7312.91	0.08
4	8178.80	0.07	8178.50	0.03	8178.50	0.02	8178.48	0.03
5	8681.71	0.05	8681.65	0.06	8681.68	0.07	8681.71	0.05
6	9293.94	0.08	9293.70	0.06	9293.68	0.04	9293.78	0.05
7	10245.60	0.03	10245.59	0.02	10245.60	0.02	10245.58	0.02

[a] One control filter measured 6 times, $n = 6$.
[b] Five filters, each measured 6 times, $n = 5 \times 6 = 30$.
[c] Standard uncertainty of the mean = standard deviation/$\sqrt{n}$.

olution on the Bruker FT spectrometer, and the resulting band locations converted to air wavelength (at nominally constant spectral slit width) for validation of the PE900 calibration.

The wavelength biases of the spectrometers were determined by fitting a linear least squares model of the (bias = certified − found) positions of the SRM 1920a and SRM 2065 standards to the found positions on the PE900 and Cary 5e instruments, for each spectral slit width. The band positions of SRM 2065 were determined using a 10% band fraction centroid method (as per the certificate[7]). The band locations of SRM 1920a were originally certified using a manual graphical extrapolated bisectional method.[13] Herein the band locations for SRM 1920a were determined by using the average of a five-point-cubic polynomial fit and the Grams/32 v7.02 (ThermoElectron, Salem, NH) peak picker. The Grams/32 algorithm is a modified center-of-gravity method employing the top three points in the peak. Typically, both an offset and slope bias were observed on the PE900, which is consistent with its use of a single point (second order D_2 line) calibration method. The raw spectra of the SRM 2036 samples were analyzed using a 10% band fraction centroid method, and the resulting band locations were corrected with the appropriate calibration (least squares bias) curve. Calibration accuracy is estimated by the instrument vendors to be ±0.3 nm for both the Cary and PE900 spectrometers. The band location uncertainty of SRM 1920 is 1 nm, while SRM 2065 varies from 0.2 nm to 0.6 nm.

The UV-Visible wavelength axis of the PE900 was calibrated using SRM 2034, the holmium oxide solution wavelength standard covering 240 nm to 650 nm.

Homogeneity Measurements. The band location homogeneity of the filters was determined by a single-pass transmission measurement on the Bruker FT instrument. The spectra of the filters were acquired in the temperature-controlled sample chamber of the spectrometer using the Pike autosampler. Six repeats of each filter were collected at 4 cm^{-1} constant resolution. A control filter, SRM 2035, was measured with the five other SRM 2036 filters during this experiment.

Band Location Algorithm: Centroid Method. The locations of the seven certified bands in SRM 2036 and SRM 2065 were determined with a center-of-gravity (hereafter referred to as centroid) approach as initially described by Cameron et al.[14] This algorithm was chosen because it has been demonstrated to provide higher precision for peak location with NIST wavelength standards than other methods that utilize curve-fitting or minimum-finding algorithms.[4,15–17] All certified bands of SRM 2036 were evaluated with a band fraction of 0.1, and these will subsequently be referred to as $^{10\%}$B locations.

RESULTS AND DISCUSSION

Homogeneity. Previous batches of this glass mixture (SRM 2035, SRM 2065) prepared by Schott were found to have no detectable filter-to-filter absorbance band location variance that could be attributable to material heterogeneity.[5] In those studies the entire SRM population (>100 filters) was measured. For this study, a subsample of 15 filters (glass only, no PTFE backing), coming from two opposite corners of the block and the center, was deemed adequate to assess the heterogeneity (if detectable) of this melt. Assessing the extent of heterogeneity of the melt via the band locations enables the use of a batch certification rather than individual certification of each SRM unit.

Table I lists the mean and its standard deviation for each band location (B_1 to B_7, obtained using the centroid method) of both the SRM 2036 set (runs 1–3, 15 filters) and the SRM 2035 control filter. The band location precision for both the single control filter and the homogeneity set is essentially the same, except for B_3 of the control filter. It is known that this band is the most affected by water vapor. Because the control filter is the first to be measured after the initiation of a run, the instrument purge is likely not as complete as for subsequent measurements, and the precision for locating B_3 on the first measurement is adversely affected. Eliminating B_3 from consideration and comparing the root-sum-of-square deviations for the remaining bands indicates that there is no difference in the precision of the measurements between the single control filter and that of the 15 SRM 2036 filters. This would suggest that no heterogeneity is detectable in the material, and thus in the band locations, at the level of the precision of the instrument measurements. As a result, all remaining certification measurements were done on randomly chosen filters cut from this melt.

Integrating Sphere Reflectance Measurement of SRM 2036 Using the BioRad FTS-60A. Data from the BioRad FTS-60A equipped with the integrating sphere

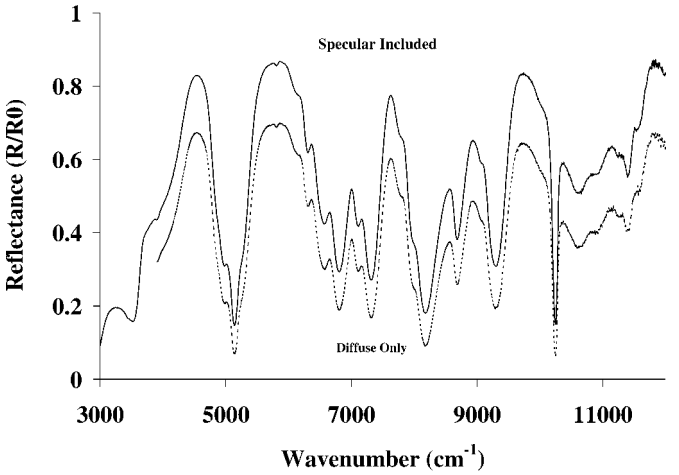

FIG. 3. SRM 2036 measured in specular-included and diffuse-only modes: BioRad FT Spectrometer.

were acquired in specular-included (using the 8° sample holder) mode for both SRM 2036 (with the PTFE backing) and a sintered PTFE reference sample. These measurements were repeated in diffuse reflectance collection only (specular-excluded) mode for SRM 2036 and the reference PTFE sample. Figure 3 compares the spectra acquired from the test samples in both collection modes.

The band locations for SRM 2036 calculated from the spectra acquired in both specular-included and diffuse-only modes on the BioRad FTS are listed in Table II. The diffuse-only data is the average of three separate experiments (including the half-block), which accounts for the higher precision of these band locations as compared to the specular-included band locations. The signal-to-noise decreases significantly in the spectral region above 8000 cm^{-1} due to the limited sensitivity of the HgCdTe detector (as is seen in Fig. 3). None of the bands show a significant bias (for this number of repeat measurements, $n = 12$), given the calculated standard errors. For the purposes of this first issuance of this standard, both modes were considered to give equivalent band locations, and the subsequent uncertainty budget reflects this. Addition of the half-blocks, for the prevention of inter-reflection, did not reveal a discernable location bias.

Fiber-Optic Bruker Measurements. For comparison to the BioRad FT, SRM 2036 was measured using the bifurcated fiber probe assembly interfaced to the Bruker IFS-66 spectrometer. This sampling configuration is commonly encountered in typical NIR applications. The reflectance spectra of SRM 2036 were acquired versus a reference spectra of a calibrated PTFE sample. Reference spectra may also be acquired from the side of the PTFE not in contact with the REO glass of the standard. However, neither of these two reference methods will compensate for the front-surface-specular component of the REO glass, and the sample reflectance measured in this mode will be >100%, due to this Fresnel reflection.

Six samples of SRM 2036 were tested in three different modes to ascertain the effect of the background/reference correction on the NIR band locations of the SRM. Mode ''B'' utilized a bare sample of PTFE as the reference. This provides no correction for the specular reflection of the REO glass. The probe was positioned above the PTFE sample so that the maximum diffusely reflected signal is obtained. Mode ''G'' utilized a 0.125 in. thick piece of borosilicate glass, physically in contact with the PTFE to attempt to compensate for the specular reflectance of the REO glass. Again, the fiber probe was positioned above the glass/PTFE sandwich to maximize the reflected signal. Mode ''C'' is representative of the most typically used position of the fiber probe, direct contact with both the REO glass and PTFE reference. This mode minimizes collection of specularly reflected light from the surface of the standard, but at the expense of the signal-to-noise ratio.

Figure 4 illustrates the effect upon the reflection spectrum of SRM 2036 using the three tested background modes. When the bare PTFE is used for background correction, the calculated reflectance–absorbance spectrum has reflectance values exceeding 300% due to the specular component of the glass filter. However, mode ''G'' (plate glass background) and mode ''C'' (direct contact) still do not entirely compensate for the specular component. Figure 5 is a plot of the bias between each of the bands with respect to the certified location (i.e., certified location minus mode × location) for each of the three modes tested. The error bars are the calculated 95% confidence intervals (see below) for each of these bands. Only B_2 and B_3, measured using the glass compensation plate, have bias outside of the 95% CI. The bias of B_3 can be explained by the effects of atmospheric water. B_2 has the largest temperature coefficient of the seven certified bands[6] and the fiber probe measurements were

TABLE II. BioRad FT integrating sphere $^{10\%}$B location. All values in cm^{-1}.

	Diffuse only[a]		Specular included[b]		Difference	
Band	$\bar{X}$	$u(\bar{X})$[c]	$\bar{X}$	$u(\bar{X})$[c]	Δ	$u(\Delta)$
1	5139.44	0.07	5139.33	0.03	−0.11	0.08
2	6804.27	0.06	6803.88	0.11	−0.39	0.13
3	7312.75	0.20	7312.55	0.14	−0.20	0.24
4	8179.03	0.09	8178.92	0.20	−0.11	0.22
5	8681.80	0.29	8682.78	0.60	0.98	0.67
6	9293.38	0.12	9293.94	0.38	0.56	0.40
7	10244.69	0.27	10244.92	0.27	0.23	0.38

[a] One filter measured in three modes: half-block included day 1, half-block excluded day 2, half-block excluded, remount filter day 3, 24 repeats each measurement, 1024 coadds each repeat.
[b] One filter measured 1 times, $n = 24$ repeats, 1024 coadds each.
[c] Standard deviation of the mean = standard deviation/$\sqrt{n}$.
[d] Standard uncertainty of the difference.

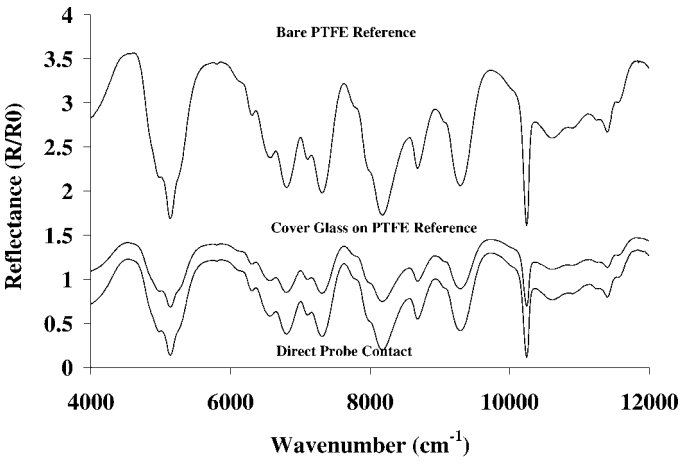

FIG. 4. Comparison of background modes for fiber probe measurements: Bruker FT spectrometer.

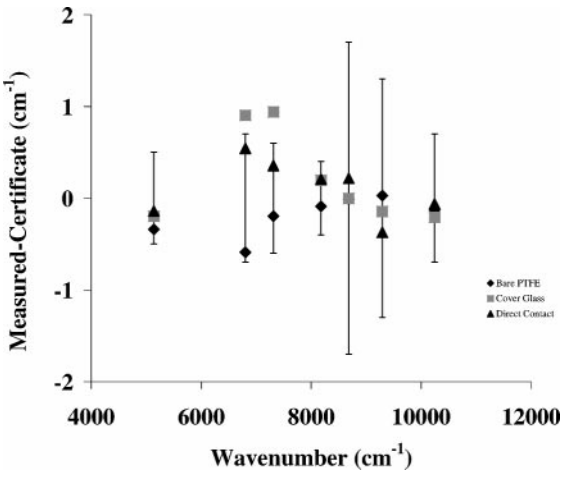

FIG. 5. Bias of the measured versus the certified reflectance 10% band locations for the three modes of reference (background) measurement using the fiber probe. The error bars represent the 95% confidence limits for the certified values of the band locations.

made at lower temperatures (21 °C vs. 24 °C) than the FT integrating sphere measurements, possibly contributing to this difference. Also the centroid method is sensitive to baseline changes that affect the start and stop points of the integration for the centroid. Trying to compensate for the specular reflection component of the REO standard with a glass that has a dissimilar refractive index and dispersion introduces a slight slope into the baseline of the mode G collected spectra. For this reason, compensation by this method is not suggested, and the PTFE in the standard is not covered/protected by a cover glass. Figure 5 demonstrates, however, that for the current levels of uncertainty in the band locations, the mode of background correction is largely insignificant.

Table III lists the average 8 cm^{-1} resolution band locations for the fiber probe measurements as a function of the mode of reference correction. In comparison to the BioRad FT data, the precision of these measurements is a factor of ten better. This is largely due to the enhanced sensitivity of the InGaAs detector versus the HgCdTe detector and the optical inefficiency of the integrating sphere used on the BioRad system.

The certified values of the vacuum wavenumber reflectance $^{10\%}$B locations of SRM 2036, listed in Table IV, were obtained by combining the Bruker fiber probe measurements and BioRad band locations. The fiber probe measurements included 60 measurements of the SRM, over a period of 10 days, using the three background correction modes previously mentioned. The certified $^{10\%}$B values are calculated as the equally weighted averages of the combined Bruker fiber probe and BioRad specular-included and diffuse-only measurements. The 95% CIs for each band are calculated using Student's T distribution with $n = 3$, representing the three modes of measurement. All uncertainties are calculated in accordance with NIST guidelines.[18] This is a conservative estimate of the uncertainty of the band location as it includes both specular and diffuse components of the reflectance and no compensation for temperature variation during these measurements.

Near-Infrared $^{10\%}$B Locations of Wavelength Dispersive Reflectance Measurements. Samples of SRM 2036 were evaluated in specular-included and diffuse-only modes on both the PE900 and Cary 5e. A calibrated Spectralon® standard was used for all reference measurements. The band locations were determined for spectral slit widths of 3 nm, 5 nm, and 10 nm between 900 nm and 2200 nm, and the certified $^{10\%}$B locations are listed in Table V. Table VI is the average difference between the specular-included and specular-excluded (diffuse-only) measurements. The bias between these two modes is well within the bias between the two reference spectrometers and therefore is included in the final location estimate for each of the bands. As a result, the band positions do not require correction for the specular component of the wavelength standard.

TABLE III. Bruker FT fiber probe measurements of SRM 2036 at 8 cm^{-1} wavenumber resolution. Comparison of $^{10\%}$Band locations as a function of background reference method. All values in cm^{-1}.

	Mode B[a]		Mode G[b]		Mode C[c]	
Band	$\bar{X}$	$u(\bar{X})$	$\bar{X}$	$u(\bar{X})$	$\bar{X}$	$u(\bar{X})$
1	5139.74	0.09	5139.60	0.07	5139.54	0.06
2	6804.49	0.14	6803.00	0.10	6803.36	0.33
3	7312.90	0.34	7311.76	0.56	7312.34	0.35
4	8179.09	0.14	8178.80	0.11	8178.79	0.17
5	8682.01	0.28	8682.00	0.17	8681.78	0.68
6	9293.87	0.28	9294.04	0.28	9294.27	0.12
7	10245.03	0.12	10245.11	0.06	10244.96	0.04

[a] Bare PTFE for reference measurement. Probe distance to sample adjusted to maximize signal. Number of measurements = 6.
[b] PTFE with cover glass for reference measurement. Probe distance to sample adjusted to maximize signal. Number of measurements = 6.
[c] Contact probe directly to SRM 2036 and cover glass to minimize collection of specular reflected light. Number of measurements = 6.

TABLE IV. Combined BioRad FT with Bruker fiber probe measurements. All values in cm^{-1}.

Band	$\bar{X}$[a]	u[b]	$\hat{u}(\bar{X})$[c]	$u(\bar{X})$[d]	$U_{95}(\bar{X})$[e]
1	5139.45	0.13	0.04	0.08	0.34
2	6803.89	0.37	0.08	0.22	0.94
3	7312.56	0.20	0.15	0.14	0.61
4	8178.94	0.08	0.13	0.08	0.36
5	8682.15	0.54	0.38	0.38	1.65
6	9293.88	0.47	0.23	0.30	1.30
7	10244.88	0.17	0.22	0.16	0.70

[a] Grand mean of the Bruker fiber probe measurements and the BioRad specular-included and diffuse-only measurements.
[b] Standard uncertainty of the Bruker fiber probe measurements and the BioRad specular-included and diffuse-only measurements.
[c] Pooled estimate of the standard uncertainty of the mean for any set of measurements.
[d] Standard uncertainty of the grand mean, $\sqrt{u(\bar{X})^2 + u^2/3}$.
[e] Approximate 95% confidence interval on the grand mean and a coverage factor of 4.3, based on Student's T-distribution with two degrees of freedom.

TABLE VI. Difference between the specular-included and diffuse component averages. All values in nm.

	(Specular Included) − (Diffuse)		
Band	3 nm SSW	5 nm SSW	10 nm SSW
7	−0.03	0.01	−0.11
6	−0.05	0.02	−0.07
5	−0.05	0.03	−0.07
4	−0.03	0.00	−0.09
3	0.00	0.04	−0.06
2	−0.04	0.03	−0.05
1	−0.02	0.02	−0.03

The certified $^{10\%}$B locations for B_1 to B_7 listed in Table V are the equally weighted means of the data obtained from the PE900 and Cary 5e measurements in both specular-included and diffuse-only modes. The standard error of the mean is also tabulated with the number of spectra contributing to the mean listed in the heading. The 95% CI for these measurements would typically be calculated using a T-statistic. The values obtained, however, are less than the 95% CI of either SRM 2065 or SRM 1920a that were used to calibrate each instrument in reflectance mode. Therefore, the lower bounds on the uncertainty of SRM 2036 were increased to match the 95% CI of SRM 2065. Work is in progress to reduce the CIs of SRM 2065 and SRM 1920a, which in turn will permit a more realistic estimate of the uncertainty for this SRM, especially for those values obtained at 10 nm SSW (where the uncertainty of B_2 is 3.7 nm). The high degree of precision capable of estimating the band locations of SRM 2036 is apparent, however, as the highest standard error of the mean for these measurements does not exceed 0.05 nm.

Information Values for the $^{10\%}$B Locations of the Ultraviolet–Visible Bands Using Wavelength Dispersive Reflectance Measurements. Many of our customers will use wavelength dispersive instruments capable of acquiring reflectance data in the region between 400 nm and 1000 nm. SRM 2036, as well as SRM 2065, has a rich UV-Visible spectrum that may be used to calibrate such instruments. Resources were unavailable for a thorough analysis of the band locations of SRM 2036 in this region, but we have performed survey scans of SRM 2036 on the PE900 using the PELA 1020 accessory in this spectral region. The spectrum of SRM 2036 acquired in specular-included mode with a 5 nm SSW versus a Spectralon reference is shown in Fig. 6. As with SRM 2065, 13 additional bands are found between 334 nm and 900 nm. The same numbering convention for SRM 2065 will be used to label the reflectance–absorptance bands of SRM 2036. The values for the $^{10\%}$B band locations of SRM 2036 in this spectral region for 5 nm SSW are listed in Table VII. No uncertainties are provided in the certificate as these are information values.[1] However, the calibration of the PE900 was validated with SRM 2034 and the internal deuterium lamp and is believed to be no worse than 0.2 nm (95% CI) from 230 nm to 850 nm.

$^{10\%}$B Locations of SRM 2036 in Transmission (Fourier Transform). SRM 2036 is not intended for use as a transmission wavelength standard. However, the composition of SRM 2036 is nearly identical to SRM 2035 and SRM 2065, and a transmission method was used to assess the homogeneity (see above), stability, and temperature coefficients of the band locations of this melt. The transmission $^{10\%}$B locations of SRM 2036 are listed in Table VIII, for comparison only, to SRM 2035 and 2065 at 8 cm^{-1} resolution. The three melts show remarkable agreement, given the complexity of the glass matrix and the four-year time period between acquisition of the melts used to produce SRM 2035 and SRM 2036. While no complex matrix glass can be a true ''intrinsic'' standard, the observed reproducibility may make this glass an attractive material for secondary standards producers. Indeed, a commercial vendor now includes a sample of this glass internally in several of their production FT-NIR

TABLE V. Combined Cary 5e and PE900 air wavelength reflectance $^{10\%}$B band values. All values in nm.

	3 nm SSW[a]			5 nm SSW[b]			10 nm SSW[c]		
Band	$\bar{X}$	$u(\bar{X})$	U_{95}[d]	$\bar{X}$	$u(\bar{X})$	U_{95}[d]	$\bar{X}$	$u(\bar{X})$	U_{95}[d]
7	976.0	0.016	0.3	976.0	0.006	0.2	975.9	0.014	0.6
6	1075.7	0.012	0.2	1075.7	0.012	0.9	1075.8	0.026	2.2
5	1151.4	0.012	0.1	1151.2	0.005	1	1151.0	0.009	3.4
4	1222.1	0.015	0.4	1222.1	0.014	0.3	1222.1	0.026	0.9
3	1367.1	0.009	0.4	1367.2	0.01	0.5	1367.3	0.023	0.2
2	1469.6	0.022	0.4	1469.6	0.019	1.7	1469.5	0.03	3.7
1	1945.7	0.042	0.3	1945.8	0.023	0.7	1945.6	0.01	1.5

[a] Mean and standard uncertainty of the mean based on $n = 57$ measurements.
[b] Mean and standard uncertainty of the mean based on $n = 42$ measurements.
[c] Mean and standard uncertainty of the mean based on $n = 24$ measurements.
[d] SRM 2065 95% confidence intervals used in the calibration of the reference instruments.

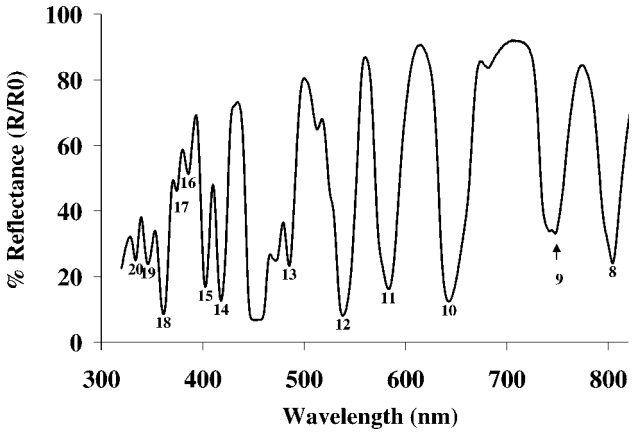

FIG. 6. UV-Visible Spectrum of SRM 2036 at 5 nm SSW.

TABLE VII. Information[a] band locations for SRM 2036 measured in reflectance at 5 nm SSW. Wavelength in nm.

Band	Wavelength
20	333.8
19	346.1
18	361.3
17	374.3
16	385.8
15	402.6
14	418.2
13	485.3
12	538.2
11	583.3
10	642.7
9	747.6
8	804.2

[a] A NIST information value is not certified and has no associated uncertainty as there is insufficient information to make an assessment of the uncertainties.

systems.[20] A list of transmission band locations of SRM 2036 for other resolutions is given in the certificate.[9]

Transmission measurements were also used to assess the temperature coefficients of the band locations of all three melts. The results of this study are detailed in a recent publication.[6] To summarize, the temperature coefficients of the NIR band locations could all be described by band-specific linear models with a unique regression-calculated slope ($cm^{-1}/°C$) and 0° intercept. The temperature coefficients (slopes) for all melts were indistinguishable. The range of temperature coefficients for the seven NIR bands for this glass composition range from a low of -0.08 $cm^{-1}/°C$ to high of 0.09 $cm^{-1}/°C$. The 0° intercepts show slight differences for each melt, which was anticipated due to the slight differences in band locations between these melts (see Table VIII).

The stability of the band locations of SRM 2036 was monitored for a period of 15 months in transmission mode. These measurements were acquired in a number of instrument states (different detector and temperatures). All bands were found to be well within the final location uncertainties, indicating that the SRM 2036 glass band locations are stable for at least the period of this certification study. This is consistent with our previous experience with SRM 2035 and SRM 2065.

SRM 1920. That several vendors now produce SRM 1920 surrogates and wish to extend the utility of this standard demonstrates the wide-spread acceptance and popularity of this material in the NIR community. To support these efforts, NIST may assess the feasibility of declaring certain bands of the SRM 1920a three-component mixture as intrinsic wavelength standards, much like a recent study involving SRM 2034.[21] SRM 2034 is a UV-Visible wavelength standard that is a 10% by weight mixture of holmium oxide in perchloric acid. With careful attention to the purity of the reagents, the band locations of this SRM have been determined to be invariant and are an intrinsic property of this mixture. SRM 1920a is a physical mixture of three neat rare earth oxides, and thus the band locations might logically be expected to also be an intrinsic property of this mixture. Providing data, rather than physical standards, will allow NIST to devote resources to other needs while providing secondary standards vendors a path for traceability.[22] Recent studies with an SRM 1920 surrogate have shown the equivalency of this approach.[1]

CONCLUSION

SRM 2036 was initially developed as a complement to NIST's SRM 1920a, and to address several shortcomings of the physical mixture of the three neat rare earth oxides. Because secondary standard producers can easily reproduce SRM 1920a, NIST will no longer produce this standard. For those requiring traceability to a National Metrology Institute, SRM 2036 exists. This standard has several demonstrated advantages over its predecessor, namely, reduced dependence of band location on system resolution; use of the same material as NIST's NIR transmission standards; certification for use with FT and dispersive instruments; and well-defined temperature coef-

TABLE VIII. Comparison of transmission band locations for SRM 2035, SRM 2065, and SRM 2036. $^{10\%}$B location for 8 cm^{-1} constant wavenumber resolution. All values are in cm^{-1}.

	SRM 2035[a]		SRM 2065[a]		SRM 2036	Combined	
Band	Value	U_{95}[b]	Value	U_{95}[b]	Value	Mean	SD
1	5138.5	0.2	5139.3	0.5	5138.5	5138.8	0.5
2	6804.6	0.3	6806.3	0.9	6804.5	6805.1	1.0
3	7313.3	0.3	7314.9	0.7	7312.9	7313.7	1.1
4	8178.7	0.2	8180.1	0.9	8178.5	8179.1	0.9
5	8682.1	0.2	8682.7	1.3	8681.8	8682.2	0.5
6	9294.0	0.3	9294.4	0.8	9293.7	9294.0	0.4
7	10245.2	0.1	10245.6	0.6	10245.5	10245.4	0.2

[a] Certified values of SRM 2035 and SRM 2065 from their respective certificates.
[b] Uncertainties represent U_{95}, the expanded 95% confidence intervals.

ficients. The glass artifact also has evaluated bands in the UV-Visible portion of the spectrum, allowing its use from 334 nm to 1950 nm.

1. T. Isaksson, H. Yang, G. J. Kemeny, R. S. Jackson, Q. Wang, K. M. Alam, and P. R. Griffiths, Appl. Spectrosc. **57,** 176 (2003).
2. H. Yang, R. S. Jackson, T. Isaksson, and P. R. Griffiths, J. Near Infrared Spectrosc. **11,** 229 (2003).
3. Schott Glass Inc., Duryea, PA, as special melt S8851.
4. S. J. Choquette, J. C. Travis, and D. L. Duewer, Proc. SPIE-Int. Soc. Opt. Eng. **3425,** 94 (1998).
5. D. L. Duewer, S. J. Choquette, L. E. O'Neal, and J. J. Filliben, Anal. Chim. Acta **490,** 85 (2003).
6. S. J. Choquette, L. E. O'Neal, and D. L. Duewer, Anal. Chem. **75,** 961 (2003).
7. Standard Reference Material SRM 2065; National Institute of Standards and Technology; Gaithersburg, MD, 2002. http://srmcatalog.nist.gov/SRM2035.
8. Standard Reference Material SRM 2035; National Institute of Standards and Technology; Gaithersburg, MD, 1999. http://srmcatalog.nist.gov/.
9. Standard Reference Material SRM 2036, National Institute of Standards and Technology, Gaithersburg, MD, USA, 2003, http://srmcatalog.nist.gov/SRM2036 Certificate of Analysis.
10. L. M. Hanssen and S. Kaplan, Proc. SPIE-Int. Soc. Opt. Eng. **3425,** 16 (1998).
11. S. L. Gilbert and W. C. Swann, ''Standard Reference Materials: Acetylene C2H2 Absorption Reference for 1510 nm–1540 nm Wavelength Calibration—SRM 2517.'' NIST special publication 260–133 (1997).
12. G. Guelachvili and K. N. Rao, *Handbook of Infrared Standards II* (Academic Press, San Diego, CA, 1993).
13. V. R. Weidner, P. Y. Barnes, and K. L. Eckerle, NBS J. Res. **91,** 243 (1986).
14. D. G. Cameron, J. K. Kauppinen, J. K. Moffat, and H. H. Mantsch, Appl. Spectrosc. **36,** 245 (1982).
15. C. Zhu and L. M. Hanssen, *11th International Conference of Fourier Transform Spectrometry, AIP proceedings 430*, J. A. de Haseth, Ed. (American Institute of Physics, New York, 1998), pp. 491–494.
16. C. Zhu and L. M. Hanssen, Proc. SPIE-Int. Soc. Opt. Eng. **3425,** 111 (1998).
17. Standard Practice for Describing and Measuring Performance of Fourier Transform Mid-Infrared (FT-MIR) spectrometers: Level Zero and Level One Tests. Annual Book of Standards 2005, vol 3.06, E1421-99, 447–458.
18. Guide to the Expression of Uncertainty in Measurement, ISBN 92-67-10188-9, 1st Ed. ISO, Geneva, Switzerland, (1993): see also B. N. Taylor and C. E. Kuyatt, ''Guidelines for Evaluating and Expressing The Uncertainty of NIST Measurement Results,'' NIST Technical Note 1297 (U.S. Government Printing Office, Washington, D.C., 1994).
19. W. May, R. Parris, C. M. Beck, J. Fassett, R. Greenberg, F. Guenther, G. Kramer, S. Wise, T. Gills, J. Colbert, R. Gettings, and B. MacDonald, *Definitions of Terms and Modes Used at NIST for Value-Assignment of Reference Materials for Chemical Measurement*, NIST Special Publication 260-136 (U.S. Government Printing Office, Washington, D.C., 2000).
20. www.brukeroptics.com, and documentation for reference standards herein.
21. J. C. Travis, J. C. Zwinkels, F. Mercader, A. Ruiz, E. A. Early, M. V. Smith, M. Noel, M. Maley, G. W. Kramer, K. L. Eckerle, and D. L. Duewer, Anal. Chem.**74,** 3408 (2002).
22. http://ts.nist.gov/traceability/.